An investigation of multi-rate sound decay under strongly non-diffuse conditions: The crypt of the Cathedral of Cadiz

An investigation of multi-rate sound decay under strongly non-diffuse conditions: the Crypt of the Cathedral of Cadiz

Francesco Martellotta[1,*], Lidia Álvarez-Morales[2], Sara Girón[2], Teófilo Zamarreño[2],

1) Dipartimento di Scienze dell'Ingegneria Civile e dell'Architettura, Politecnico di Bari, via Orabona 4, I-70125 Bari, (Italy).

2) Instituto Universitario de Arquitectura y Ciencias de la Construcción (IUACC), ETSA, Universidad de Sevilla, Av. Reina Mercedes, 2, 41012 Seville (Spain).

Abstract

Multi-rate sound decays are often found and studied in complex systems of coupled volumes where diffuse field conditions generally apply, although the openings connecting different sub-spaces are by themselves potential causes of non-diffuse behaviour. However, in presence of spaces in which curved surfaces clearly prevent diffuse field behaviour from being established, things become more complex and require more sophisticated tools (or, better, combinations of them) to be fully understood. As an example of such complexity, the crypt of the Cathedral of Cadiz is a relatively small space characterized by a central vaulted rotunda, with five radial galleries with flat and low ceiling. In addition, the crypt is connected to the main cathedral volume by means of several small openings. Acoustic measurements carried out in the crypt pointed out the existence of at least two decay processes combined, in some points, with flutter echoes. Application of conventional methods of analysis pointed out the existence of significant differences between early decay time and reverberation time, but was inconclusive in explaining the origin of the observed phenomena. The use of more robust Bayesian analysis permitted the conclusion that the late decay appearing in the crypt had a different rate than that observed in the cathedral, thus excluding the explanation based on acoustic coupling of different volumes. Finally, processing impulse responses collected by means of a B-format microphone to obtain directional intensity maps demonstrated that the late decay was originated from the rotunda where a repetitive reflection pattern appeared between the floor and the dome causing both flutter echoes and a longer reverberation time.

Keywords: non-diffuse sound propagation, multi-rate decay, flutter echoes, sound focussing surfaces

Please cite this paper as: F. Martellotta, L. Álvarez-Morales, S. Girón, T. Zamarreño, An investigation of multi-rate sound decay under strongly non-diffuse conditions: The crypt of the Cathedral of Cadiz, Journal of Sound and Vibration, Volume 421, 2018, 261-274, https://doi.org/10.1016/j.jsv.2018.02.011

* Corresponding author: francesco.martellotta@poliba.it

1. Introduction

Multi-rate sound decays, that are typically observed in presence of coupled volume geometries, have received considerable attention in recent decades for acoustic design of modern performance venues [1-3]. In fact, non-exponential sound-energy decays can contribute to control reverberation and clarity of the hall [4].

The interest in coupled volume acoustics dates back to the 1950s [5] and has subsequently received several theoretical developments based on the use of statistical acoustics (SA) theory [6-8]. Recently, such theoretical approaches have been further refined and generalized [9] to address direct sound radiation and non-diffuse transfer of energy between sub-rooms. Other revisions to the improved statistical-acoustics model have later been published by the same authors [10,11]. Applications of the diffusion equation [12] as well as of geometric acoustics methods [13,14] to model coupled-room phenomena can be accounted.

In parallel to the above studies, several research efforts investigated both subjective effects [15,16] and methods to identify and quantify the different components in multi-rate decays. Several measures of double slope effect or ratios between different portions of decay were used in the literature [17-19] to describe the slope variation as a function of time. However, only the application of Bayesian methods to multi-rate decay time evaluation provided the most rigorous instrument for analysing acoustically coupled spaces [20-23].

The above mentioned models and methods of analysis successfully contributed to explain the experimental results of various acoustic parameters measured in large, and complex, spaces. Anderson and Bratos–Anderson [24] extended the original SA two-room model to a larger number of sub-rooms and applied this method to St Paul's Cathedral, London. Similarly, Martellotta used Bayesian analysis [20] and SA models [9] to explain and model the acoustics of St. Peter's Basilica [25], and of a larger set of Papal Basilicas [26] in Rome, within the framework of coupled volumes. Chu and Mak [27], and Martellotta [28] proposed the use of multi-rate decays to predict the early sound energy decay performance in churches. All the previous analyses involved spaces where, despite their complexity, sound propagation complied with diffuse field specifications, otherwise SA model would not have been valid nor accurate. However, multiple-rate decays may also appear under different circumstances, such as in long enclosures [29], in spaces with non-uniform sound absorption distribution [30], and in presence of curved and focussing surfaces [31]. In all of these cases the sound field can hardly be considered diffuse, and together with multiple-rate decays, strong non-uniform sound pressure level distribution, and odd phenomena like coloration and "flutter echoes" may appear. With particular reference to the effect of curved surfaces there are some theoretical studies [32,33], but limited measured data can be found [31] and analyses are carried out only by means of conventional methods.

In the present paper, the case of the crypt of the cathedral of Cadiz in southern Spain, is investigated. Due to its shape, a circular rotunda covered with a low dome, connected to radial galleries, this space presents almost unique acoustic features, including non-linear decays and flutter echoes, which would be difficult to analyse and explain using conventional methods. Consequently, non-linear decays were first investigated by means of Bayesian analysis to identify the different components. As this space is directly connected to the cathedral, the origin of the multi-rate decay was investigated either by comparing decay rates pertaining to different sub-volumes and by taking advantage of visualization techniques based on the use of B-format impulse responses [34]. The latter

technique also allowed to clearly explain the origin of the flutter echoes. Results are discussed below and proved that only the use of both Bayesian methods and intensity maps allowed the correct interpretation of the phenomena which, using conventional approaches might have been explained in a different, and probably incorrect, way.

2. Methods

2.1. The case study

The cathedral of Cadiz, located in the historical center of the southernmost city of Spain, is one of the cathedrals more recently built in the country. The long duration of its construction process, which began in 1722, involved seven master architects, a fact that resulted in a combination of different architectural styles: Baroque and Rococo in the interior, and Neoclassicism in the façade and the two towers. The main space of the cathedral has a Latin cross plan surrounded along its entire perimeter by lateral chapels and organized in three naves, creating an interior volume of about 70,000 m^3. Its structure is made up of Corinthian marble columns, from which a second body of limestone pillars emerges, concluded by very lightly decorated vaults. The choir is characterized by stalls made of cedar and mahogany and is one of the key elements of the building, being located in the central nave and subdividing the space. The southern part of the church includes an ambulatory and the presbytery covered with a dome. A gilded bronze pulpit is located on each side of the altar (Fig. 1a). The crypt is located right under the main altar, below sea level. The crypt, which was built by Vicente de Acero in 1730, is almost entirely finished in oyster stone, a brown porous stone typical of the region. The space, having a volume of approximately 3,000 m^3, is formed by a central vaulted rotunda, which reaches a height of 5 m in its highest point (Fig. 1b), and five axial galleries with a flat low ceiling (Fig 2). The crypt is connected to the cathedral by means of stairs arranged symmetrically on both sides of the main altar and also by means of several small openings around the rotunda (Fig. 1b).

a)  b) 

Fig. 1. Interior view of the presbytery of the cathedral of Cadiz (a) and interior view of the rotunda of the crypt (b).

2.2. Measurement technique

The measurement methodology applied to record and analyse the room impulse responses followed the recommendations listed in the ISO 3382-1:2009 standard [35] and the specific guidelines published for this type of buildings [36,37]. Such methodology has been applied in order to analyse the current acoustic environment of several Spanish cathedrals of the same

typology [38]. Considering the various liturgical and cultural uses of the churches, different sound-source positions were set. Typical source positions included the high altar, the pulpit, the choir, the organ position, and the retro-choir. For the purpose of the present paper, the crypt was also analysed in detail by taking into account two source positions, one at the altar (S1), and one in the rotunda (S2). However, some of the measurements in the main cathedral volume were also considered to better understand the results in the crypt. Receivers were also distributed to represent different homogeneous areas both in the worship area and in the crypt of the cathedral. In particular, in the crypt, receivers were distributed throughout the rotunda, and also in each radial gallery (one position was set close to the opening and the other well inside each sub-volume). A summary of the different source and receiver positions is given in Fig. 2.

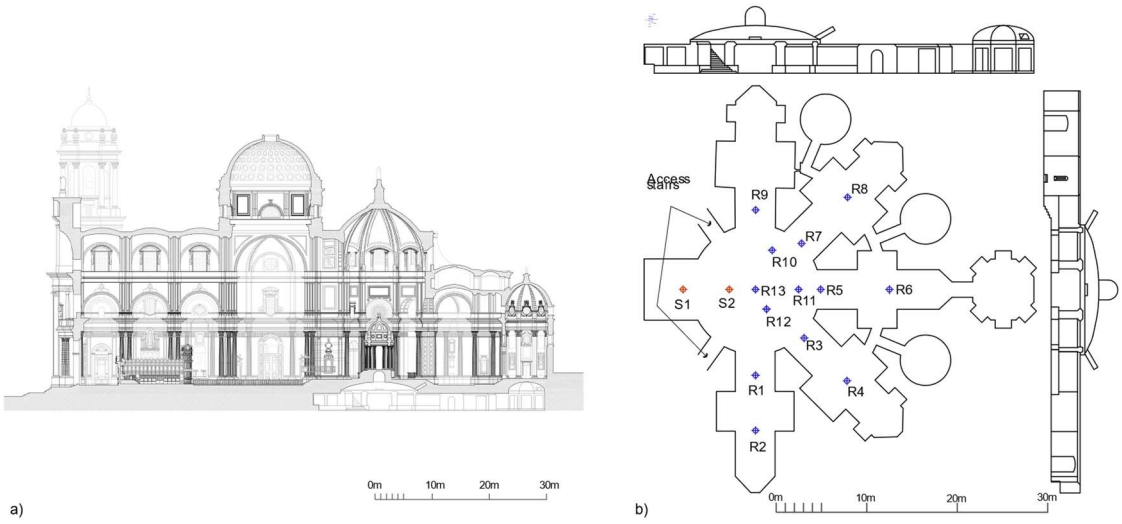

Fig. 2. a) Longitudinal sections of the cathedral and its crypt. b) Schematic plan and cross-sections of the crypt, with indication of source (S) and receiver (R) locations.

The process of generation, acquisition, and analysis of the signal was performed using WinMLS2004 software for the worship areas of the cathedral and EASERA v.1.2 software for the crypt, which were connected with the measurement chain through an Edirol UA-101 sound card. All the room impulse responses (IRs) were recorded at a sample rate of 48 kHz and 16-bit depth. The software tools used a swept-sine technique, emitted through an AVM DO-12 dodecahedral sound source with a B&K 2734 power amplifier, and a Behringer Eurolive B1800D-Pro self-amplified subwoofer, in order to improve the signal-to-noise ratio at low frequencies. A single output channel was used since the signal is sent to the subwoofer, which is self-powered and has a high-pass filter (cut-off frequency at 90 Hz) that allows the signal to be sent up to the dodecahedron. The duration of each single sweep was set at 22 s (much longer than the longest reverberation time expected in the crypt, so to ensure that harmonic distortions can be removed from measured IRs). A frequency-weighted log-sweep, spanning between 20 Hz and 20 kHz, was used as excitation signal, so to achieve an almost flat spectrum that enables the best performance of the subwoofer and the dodecahedron without exciting non-linear behaviour. The software recorded the monaural IRs through an Audio-Technica AT4050/CM5 omnidirectional/figure-of-eight microphone whose amplifier and polarization source is a SMP200 Sound Field. Binaural IRs were measured with a Head Acoustics HMS III dummy head connected to a B&K-2829 power

supply. Moreover, B-format IRs were registered by using a MK-V SoundField microphone. This measurement chain complies with the "advanced" set-up proposed in Ref. 36. Measurements were carried out at night, when the church was unoccupied and the background noise was at a minimum (equivalent sound levels of 28.7 dBA and 26.7 dBA were recorded in the main church and crypt, respectively). Furthermore, environmental conditions were monitored, with average values of 22ºC and 76% RH.

2.3.Methods of analysis

In order to analyse the measured decays, several techniques were used. First, Bayesian analysis [20-23] was chosen as it provides the most rigorous method to detect and quantify multiple slopes in decays. According to Bayesian analysis, any decay curve can be expressed in terms of a multi-rate decay process given by the sum of different components:

$$F(A,B,t_k) = A_0(L-t_k) + \sum_{i=1}^{n} A_i \exp(-B_i t_k), \text{ with } 0 \le t_k \le L, \quad (1)$$

Where n is the decay order, t_k is the time step, L is the total duration of the decay, A_i is the "linear parameter" representing the amplitude of the i-th decay, B_i is the "nonlinear parameter" equal to $13.8/T_i$, with T_i being the i-th reverberation time to be estimated. Finally, A_0 is the amplitude of the background noise component of measured IRs. The scope of Bayesian analysis is to determine the set of A_i and B_i parameters which best describes the decay curve.

Among the many algorithms developed in the last years [20-23], the fully parametric one proposed by Xiang et al. [23] was implemented in Matlab. Even though the procedure may be applied to a virtually unlimited number of slopes, for the IRs under test only double and triple slopes were considered.

In order to use a single number parameter to compare the energy associated to different decays, the logarithmic ratio of the amplitudes $A_{ij}=10\cdot\log_{10}(A_i/A_j)$ was used in the manuscript. Finally, to limit lengthy discussions and be consistent throughout the different sections of the paper, the 125 Hz, 500 Hz, and 2 kHz octave bands were considered. However, similar results were obtained at the other bands.

3. Experimental results

3.1. Conventional analysis

The analysis of the acoustical parameters measured in the crypt pointed out interesting differences depending on source and receiver positions (Table 1). When the source was in the rotunda (S2) longer EDT and T30 values were measured at the receivers located in the same sub-volume (R10-R13). Listening to impulse responses (IRs), and observing decay curves, showed that such an effect was associated with a very audible flutter echo (Fig. 3). The origin of such flutter echoes (having a period of about 0.2 s, depending on the receiver, corresponding to a roundtrip path of about 70 m) was originally attributed to reflections between the opposite ends of the galleries. However, thanks to the more sophisticated analysis, it was demonstrated that, as will be better explained below, they depended on the curved surfaces (walls and vault) of the rotunda. When receivers were located in the adjacent sub-volumes (R1-R9), EDT values spanned between 1.4 and 2.1 s at 500 Hz octave band, while T30 values spanned between 2.9 and 3.4 s. At different octave bands slightly shorter values were generally observed, with EDT being shorter than T30 in any case. When the source was moved to the altar (S1) a significant change occurred, with EDT decreasing nearly everywhere (spanning from 0.9 to 1.6 s at 500 Hz octave band) and

T30 varying between 3.1 and 3.9 s in the rotunda, and dropping to about 1.45 s (spanning from 1.4 and 1.5 s) in the galleries. Substantially similar trends were observed at other octave bands.

Table 1.
Summary of EDT and T30 values measured at the 125 Hz, 500 Hz, and 2 kHz octave bands for all source and receiver combinations located in crypt. S1 = source position at the altar; S2 = source position in the rotunda.

	125 Hz		500 Hz		2 kHz			125 Hz		500 Hz		2 kHz	
S1	EDT	T30	EDT	T30	EDT	T30	S2	EDT	T30	EDT	T30	EDT	T30
R1	1.37	1.41	1.28	1.42	1.18	1.33	R1	1.70	1.63	1.91	3.42	1.50	2.43
R2	1.49	1.58	1.60	1.47	1.25	1.42	R2	1.39	2.02	2.16	3.07	1.48	2.32
R3	1.64	1.39	1.25	1.45	1.05	1.31	R3	0.88	1.66	1.74	3.49	1.53	2.52
R4	1.01	1.58	1.22	1.44	1.19	1.35	R4	0.77	1.93	1.79	3.51	1.34	2.49
R5	0.98	1.34	0.89	1.36	1.12	1.32	R5	1.55	2.21	1.76	2.99	1.09	2.09
R6	1.24	1.22	1.08	1.43	1.12	1.26	R6	0.89	1.92	1.45	2.92	1.29	2.30
R7	1.27	1.40	1.20	1.44	1.07	1.33	R7	1.01	1.61	1.54	3.40	1.56	2.49
R8	1.16	1.43	1.14	1.38	1.07	1.36	R8	0.94	1.62	1.72	3.08	1.45	2.38
R9	1.52	1.60	1.23	1.44	1.06	1.33	R9	1.76	1.94	1.86	2.82	1.55	2.44
R10	1.70	2.29	1.57	3.70	1.31	2.62	R10	2.15	3.45	3.82	4.92	2.43	3.17
R11	1.36	2.38	1.40	3.11	1.19	2.47	R11	2.05	3.23	3.85	4.35	2.74	2.83
R12	1.28	2.51	1.48	3.87	1.47	2.82	R12	2.77	3.17	3.99	4.54	2.44	3.33
R13	1.40	2.27	1.54	3.00	1.42	2.23	R13	1.41	2.89	3.28	3.97	2.08	2.85

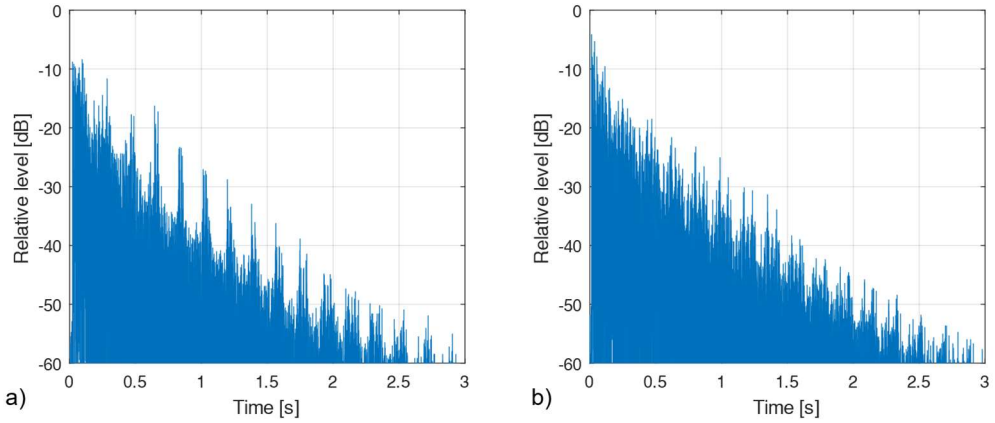

Fig. 3. Plot of relative level (wide band) as a function of time for receivers S2-R11 (a) and S2-R12 (b) showing the flutter echo appearing in the rotunda.

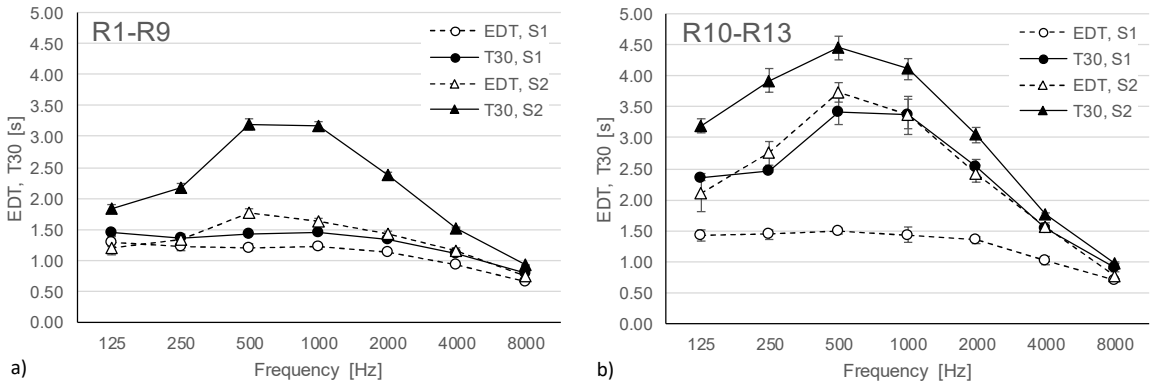

Fig. 4. Graphs of EDT and T30 values as a function of frequency and source position and receiver location: a) average of receivers located in the galleries (R1-R9); b) average of receivers located in the rotunda (R10-R13). Error bars correspond to standard deviation across measured values.

As shown in Fig. 4, the behaviour observed at 500 Hz also appears at other frequencies. In particular, when the source is at S1, EDT and T30 are rather similar inside the galleries, while in the rotunda EDT remains more or less the same, while T30 increases significantly, with the largest values observed at mid frequencies. When the source is in the rotunda (S2), EDT remains nearly the same as before in the galleries, while T30 becomes longer across the entire spectrum, with mean values very similar to those observed in the rotunda with source S1. In the rotunda, both EDT and T30 values get longer, with T30 approaching 4.5 s at 500 Hz. EDT values are quite similar to T30 values observed when the source is in position S1.

Table 2.
Summary of mean (M) and standard deviation (SD) for EDT and T30 values measured in the cathedral, at octave bands from 125 Hz to 4 kHz as a function of source position. #R indicates the number of receivers used in the calculation.

			T30						EDT					
Source	#R		125	250	500	1000	2000	4000	125	250	500	1000	2000	4000
Altar	(14)	M	11.70	11.29	9.88	7.90	5.88	4.18	11.30	11.03	9.62	7.62	5.58	3.80
		SD	0.09	0.04	0.04	0.01	0.01	0.01	0.17	0.21	0.13	0.08	0.07	0.07
Pulpit	(11)	M	11.72	11.14	9.82	7.87	5.83	4.13	11.16	11.11	9.54	7.38	5.40	3.57
		SD	0.06	0.04	0.03	0.02	0.02	0.02	0.23	0.17	0.11	0.13	0.12	0.16
Choir	(7)	M	11.67	11.19	9.84	7.83	5.78	4.08	10.02	10.51	9.01	7.09	5.11	3.46
		SD	0.14	0.03	0.03	0.09	0.07	0.10	1.58	0.74	0.68	0.73	0.70	0.47
Retro-choir	(4)	M	11.20	10.87	9.49	7.33	5.28	3.51	6.33	5.84	5.50	4.18	3.09	2.28
		SD	0.17	0.12	0.05	0.08	0.07	0.09	1.16	0.50	0.32	0.27	0.19	0.16
Organ	(3)	M	11.66	11.16	9.70	7.80	5.77	4.11	9.95	9.14	7.95	6.35	4.68	3.12
		SD	0.10	0.10	0.07	0.08	0.12	0.15	2.49	2.39	2.36	1.83	1.37	0.86

The analysis of the same parameters measured in the cathedral (Table 2) showed that T30 values are very consistent throughout the church with negligible spatial variations. As expected, EDT values showed a much larger variation, with the shortest values observed when both source and receivers were in the retro-choir. Over the entire octave-band spectrum, both EDT and T30

values measured in the cathedral were significantly longer than those measured in the crypt. Thus, conventional analysis based on classical acoustic parameters provided a first set of clues, but a more refined analysis was required in order to draw conclusions.

3.2. Bayesian analysis

Bayesian analysis allows the actual time constant of each decay process to be estimated, together with its relative amplitude. Before delving into a detailed analysis of the different cases, it is worth presenting an overview of the whole set of decay curves as a function of octave band and source and receiver position (Fig. 5). For the sake of brevity, only octave bands of 125, 500, and 2000 Hz were considered. As already appeared discussing T30 and EDT, receivers could be divided into two subsets, those located in the galleries (with little differences between those located at the opening and those deeper into the galleries), and those in the rotunda. Among the latter group, when source was in S2, the stepped decay typical of flutter echoes was observed, particularly at receivers R11 and R12. In addition to flutter echoes, variations in the energy of the late decays appeared as a function of source position. In fact, at medium and high frequencies the second decay was more energetic for source S2, while it was weaker for source S1. This was consistent with the pattern observed for T30 as a function of source position.

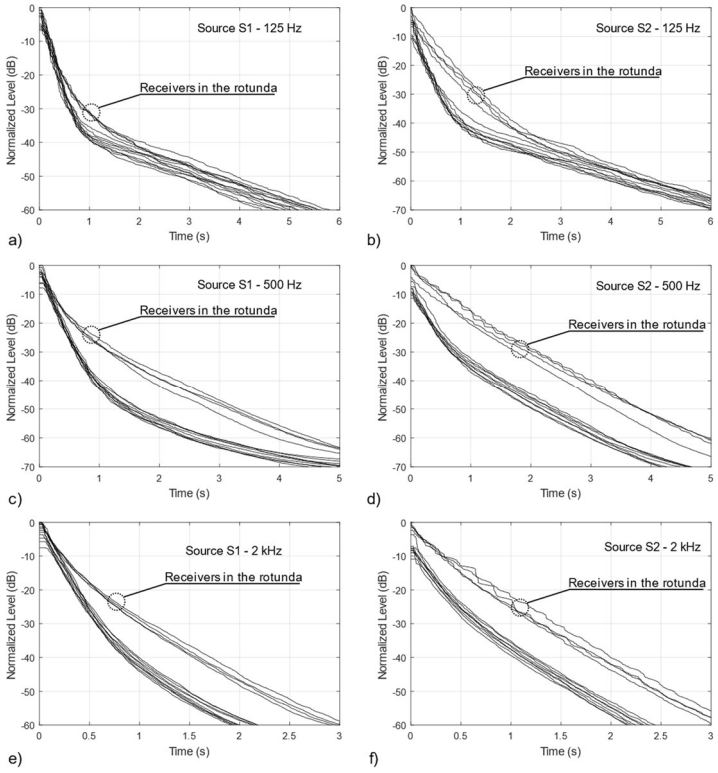

Fig. 5. Normalized backward integrated decay curves as a function of source and receiver position and octave band frequency. Normalization is obtained in each case by assuming receiver with highest relative level as a reference. a) Source S1, 125 Hz octave band; b) Source S1, 500 Hz octave band; c) Source S1, 2 kHz octave band; d) Source S2, 125 Hz octave band; e) Source S2, 500 Hz octave band; f) Source S2, 2 kHz octave band.

At the 125 Hz octave band the second decay had a slower decay rate and was more or less the same at all receivers (also having approximately the same energy both in the rotunda and in the galleries), and appeared between 30 and 40 dB below direct sound. The initial decay was relatively similar among all the receivers for source S1, while it differed for source S2 as receivers in the rotunda showed a slower decay rate with a stepped shape.

At the 500 Hz octave band, when source S2 was used, receivers in the rotunda showed an apparently linear behaviour, but Bayesian analysis will show that two slopes can still be identified. Receivers in the galleries showed a second slope which resembled that observed in the rotunda, and a first slope which was much steeper. For source S1 the second decay had weaker initial energy, likely because when source was in this position a larger amount of acoustic energy could escape in the galleries being absorbed. In addition, the slope in the galleries showed an initial steep part up to about 0.8 s, followed by a short part (between 1 and 2 s) with a slope similar to that observed into the rotunda, finally followed by an even slower decay, thus suggesting a possible third slope.

Finally, at the 2 kHz octave band the same trends observed at the 500 Hz octave band were found, although with faster decay rates. However, for source S1 the second slope seemed more similar both in the rotunda and in the galleries, where no third slope could be identified in this case.

Considering the clustering observed above, and the relatively small standard deviations observed among EDT and T30 values in Section 3.1, Bayesian analysis was applied only to four source-receiver combinations, corresponding to both source positions, and two of the most representative receivers located respectively in the galleries and in the rotunda. In the light of the strong frequency-dependent variation observed in Fig. 5 the analysis was performed at the frequency bands of 125 Hz, 500 Hz, and 2 kHz. A summary of the results is shown in Table 3.

Table 3.
Summary of T1, T2 and T3 (when applicable), and A_{12} and A_{23} values measured at 125 Hz, 500 Hz, and 2 kHz octave bands for the selected source receiver combinations.

		S1-R2			S1-R10			S2-R2			S2-R10	
	i	1	2	3	1	2	3	1	2	3	1	2
125 Hz	Ti [s]	1.35	11.4		1.45	4.0	10.1	1.53	11.15		3.33	11.4
	A_{ii+1} [dB]	23.2			15.5	8.2		22.1			27.1	
500 Hz	Ti [s]	1.45	4.65	10.3	1.78	5.45	10.1	1.85	5.31	10.1	3.44	5.89
	A_{ii+1} [dB]	24.3	11.0		10.8	18.4		12.7	23.0		2.9	
2 kHz	Ti [s]	1.23	3.43		1.08	2.95	5.3	1.49	3.47		1.53	3.54
	A_{ii+1} [dB]	19.2			5.0	16.7		9.0			1.6	

First the combination with the source at the altar and the receiver in one of the galleries (S1-R2) was analysed (Fig. 6a). Results showed that at 125 Hz two slopes were identified. The first having a reverberation time T1=1.35 s, and the second having T2=11.4 s, with A_{12}=23.2 dB. A comparison with Table 2, suggests that the second slope might be related to the reverberation time observed in the cathedral volume. As supposed observing Fig. 5, at 500 Hz three decays appeared. The first with T1=1.45 s, the second with T2=4.65 s, and the third with T3=10.3 s.

At this octave band, the third decay process, although being very weak, was similar to that taking place in the cathedral volume (Table 2), thus, suggesting that the energy radiating into the cathedral and coming back into the crypt was much weaker than at 125 Hz, and, in addition, a

new, louder, decay process appeared, whose origin will be better investigated below. Finally, at 2 kHz octave band two slopes appeared, the first having T1=1.23 s, and the second having T2=3.43 s. The latter was shorter than values measured in the cathedral, thus suggesting that the origin must be related to the crypt characteristics.

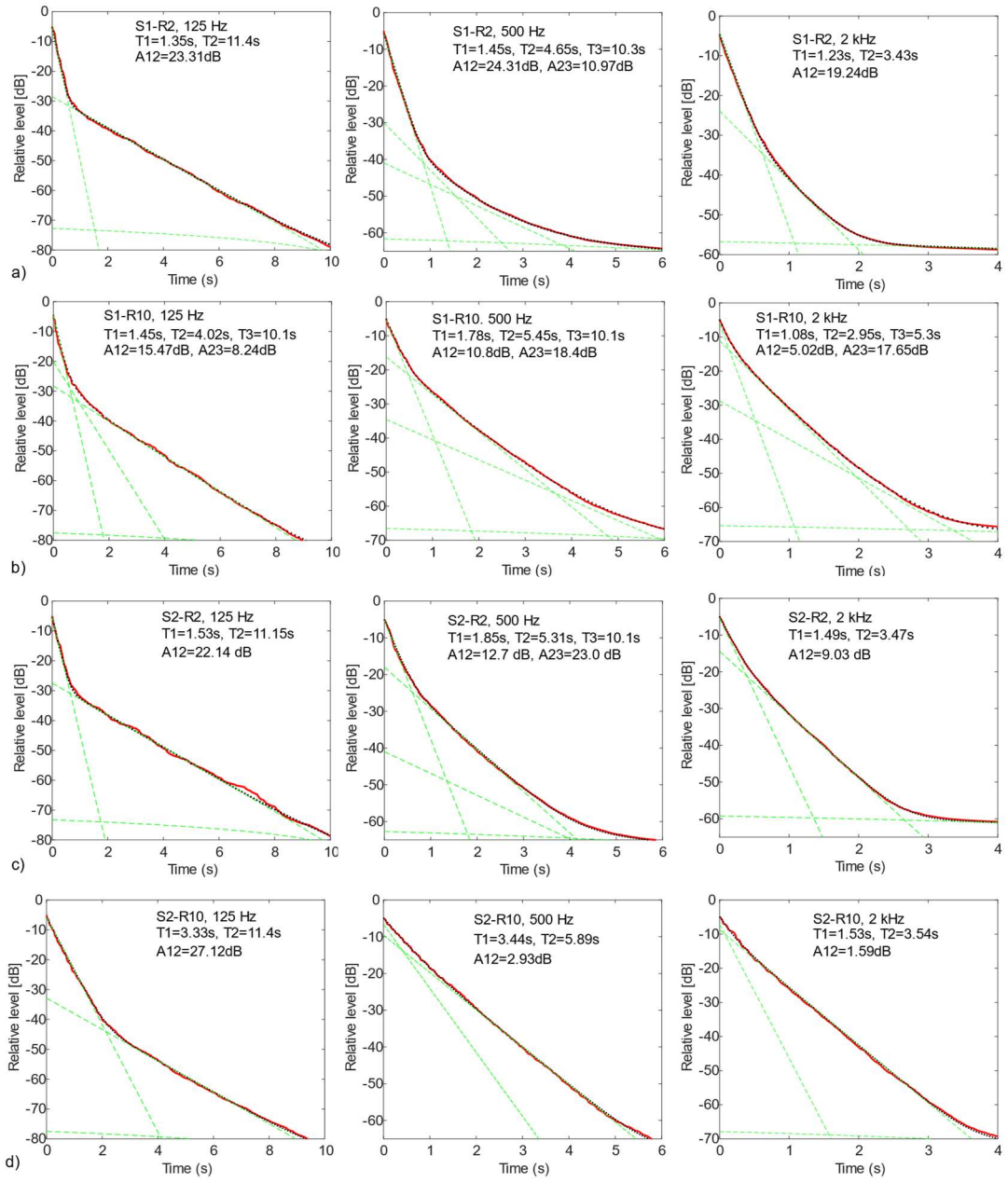

Fig. 6. Results of Bayesian analysis applied to 125 Hz, 500 Hz, and 2 kHz octave bands, at combinations: a) S1-R2; b) S1-R10; c) S2-R2; d) S2-R10. (—) Measured decay; (…) Bayesian decay; (- - -) Bayesian decay components.

When combination S1-R10 (Fig. 6b) was considered, several similarities to S1-R2 were found, although with some important differences. At 125 Hz three slopes appeared, with T1=1.45 s, T2=4.0 s, and T3=10.1 s. The third decay again showed consistent similarities with the reverberation time of the cathedral, while the second decay, making a smoother transition from the first to the third, required some further investigation. At 500 Hz, three slopes appeared with T1=1.78 s, T2=5.45 s, and T3=10.1 s. The second decay was about 14 dB louder than it was in R2, with a slightly longer reverberation time. The third decay was 7 dB louder than it was in R2, but the reverberation time was essentially the same, confirming an influence from outside the crypt. At 2 kHz, three decays appeared with T1=1.41 s, T2=3.45 s, and T3=5.7 s. The second was almost coinciding with the second decay observed in R2, while the third decay showed some similarities with that observed in the cathedral, thus suggesting a possible contribution from that volume.

When combination S2-R2 was considered (Fig. 6c), at 125 Hz, nearly the same behaviour found in S1-R2 was observed (T1=1.53 s, T2=11.15 s, and A12=22.2 dB). This seemed to suggest that at the lowest frequencies galleries behave in the same way, independent of source position. At 500 Hz three slope appeared, with T1=1.85 s, T2=5.3 s, and T3=10.1 s. The values were quite similar to those observed in combination S1-R10, suggesting that, although with minimal energy, late sound might enter the crypt from the cathedral. At 2 kHz only two decays appeared with T1=1.49 s, and T2=3.47 s, again with great similarity with S1-R10, even in terms of A_{12}.

Finally, combination S2-R10 was considered (Fig. 6d). At the 125 Hz octave band two slopes appeared, with T1=3.33 s, T2=11.4 s, and A_{12}=27.1 dB. Thus, while the late decay may be interpreted as the contribution from the cathedral, the first decay showed a clearly longer reverberation time than it was in the same position with source S1. It is interesting to observe that there was no evidence of this slower decay rate in the other combinations observed. At the 500 Hz octave band two slopes appeared with T1=3.44 s, T2=5.89 s, and A_{12}=2.94 dB, confirming that the two slopes can be identified using Bayesian analysis, but the second played a major role. The decay rate was nearly the same as was found at the 500 Hz octave band in all the other combinations. Similarly, at the 2 kHz octave band reverberation times were T1=1.32 s, T2=3.46 s, and A_{12}=0.4 dB, thus confirming that the two decay processes had nearly the same energy and consequently the slowest tended to mask the other.

At this point, in order to better understand the origin of the different decays and, in particular, to identify those pertaining to the cathedral, Bayesian analysis was extended to a sample of IRs measured with both source and receivers in the cathedral. Reverberation times (T30) in the cathedral were systematically longer than those appearing in the crypt, with the only exception of the 125 Hz octave band and the third decay appearing, with very low energy, at 500 Hz, while some similarities appeared between the second decays and EDT values measured in the retro-choir. As the crypt openings are connected directly with side aisles, it was worth investigating in greater detail what happens in those sub-spaces, and hence two IRs measured with both source and receiver in the retro-choir and organ aisle were considered. Bayesian analysis clarified (Fig. 7) that in both cases the initial decay had shorter reverberation time T1 (3.52 s at 500 Hz, and 2.0 s at 2 kHz) and an initial energy that only moderately exceeded the energy of the late decay, meaning that after less than 1 s the first decay process was completely masked by the second slower decay. Thus, it could be excluded that the origin of the decay appearing in the crypt at 500 Hz and 2 kHz might be related to the main volume of the cathedral.

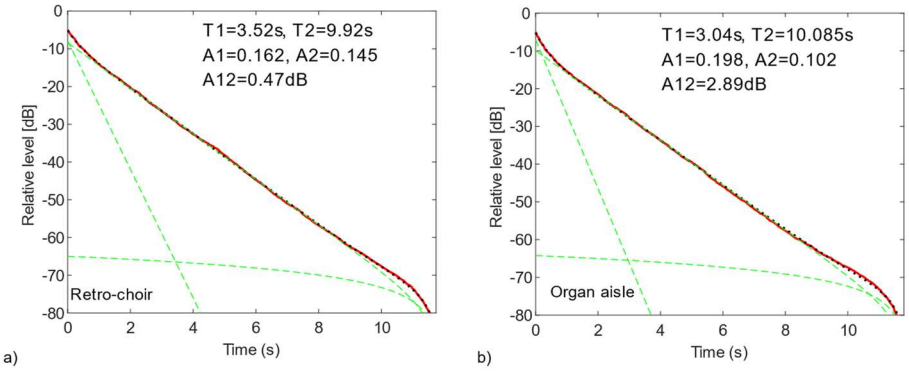

Fig. 7. Results of Bayesian analysis applied to 500 Hz octave band, at combinations corresponding to both source and receiver in the same subspace of the cathedral: a) retro-choir; b) organ position. (—) Measured decay; (…) Bayesian decay; (- - -) Bayesian decay components.

3.3. Directional maps

In order to analyse in greater detail the decay process, directional intensity maps were created [34], taking advantage of B-format impulse responses available at each receiver position. Such maps provide, for the selected time interval, a level distribution that accounts for the integral of the reflections arriving from a given direction. Thus, higher levels may result from either stronger reflections or a large number of weaker reflections. To simplify localization of direction of arrival of sounds, panoramic images were obtained using the SketchUp model of the Crypt.

First of all combination S2-R10 was analysed, because according to Bayesian analysis the late decay processes showed the maximum energy in the rotunda, thus suggesting it might have an important role. At the 500 Hz octave band, as already observed, in the early part of the impulse response several flutter echoes appeared, and the directional maps showed (Fig. 8a) that reflections between the floor and the dome were responsible for such behaviour. The process continued, as it can be observed by properly zooming into the late part, so that even after 3 s the sound field remained clearly non-diffuse.

As shown in Fig. 8b, the loudest late reflections kept coming from above and from below, while the energy coming from the horizontal plane was more than 20 dB weaker. The distribution remained approximately the same even after 5 s, confirming that when the source was in the rotunda the sound field was strongly non uniform.

Similar results were observed at receiver R11, which, being located along the symmetry axis, was also more likely to show odd behaviours. In fact, an even more evident flutter echo appeared, in which each sequence included one reflection from the floor, and two from the dome (one from front and one from the back), mostly aligned along the symmetry axis (Fig. 9a-d). The late part (Fig. 9e) was again characterized by a strongly non-uniform behaviour, with late reflections coming from the horizontal plane being much weaker than the others.

When the source was moved into the altar area (S1), flutter echoes disappeared, and the early sound field appeared more evenly diffused (Fig. 10a). However, in the late part, from 1 s onward, the sound field showed again a prevailing contribution of reflections coming from above and from the floor (Fig. 10b), suggesting that, although with a lower intensity, the non-uniform distribution of sound inside the rotunda always occurred.

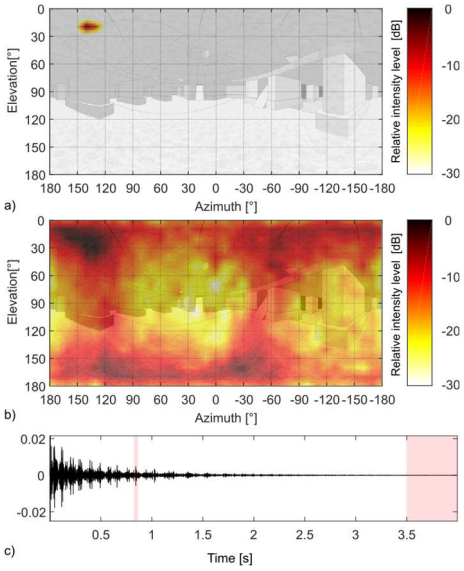

Fig. 8. Comparison between directional reflection maps at 500 Hz for combination S2-R10 at: a) 0.840 s from direct sound 10 ms time window; b) 3.50 s from direct sound 0.5 s time window. c) Impulse response (omnidirectional) with shaded areas indicating the time intervals used in a) and b). IR amplitude is expressed using arbitrary units.

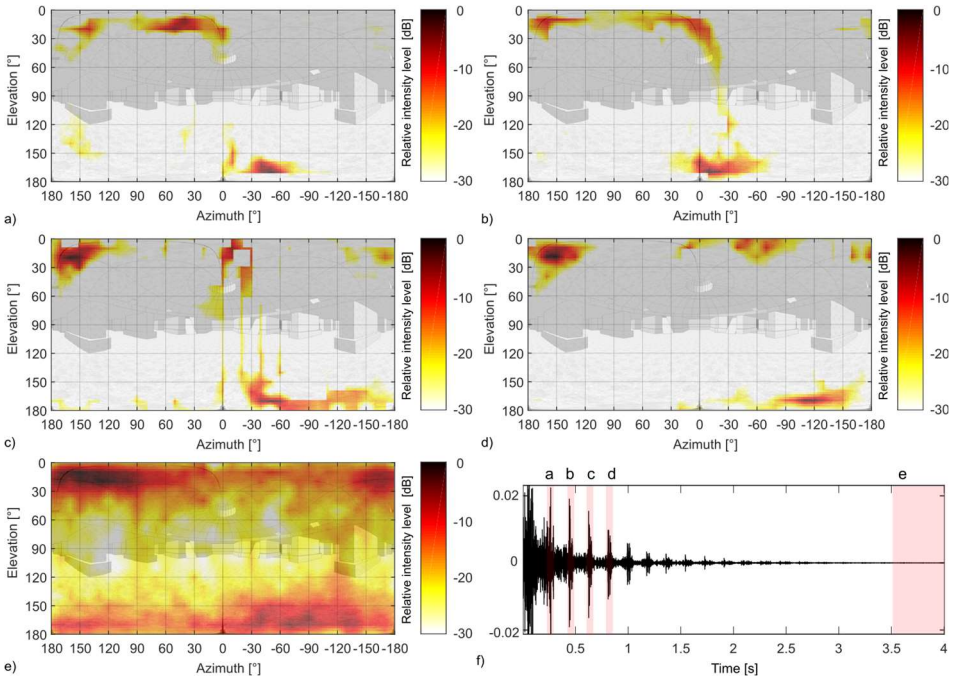

Fig. 9. Comparison between directional reflection maps at 500 Hz for combination S2-R11 at: a) 0.259 s from direct sound 50 ms time window; b) 0.438 s from direct sound 50 ms time window; c) 0.620 s from direct sound 50 ms time window; d) 0.805 s from direct sound 50 ms time window;e) 3.50 s from direct sound 0.5 s time window. f) Impulse response (omnidirectional) with shaded areas indicating the time intervals used in panels a-e. IR amplitude is expressed using arbitrary units.

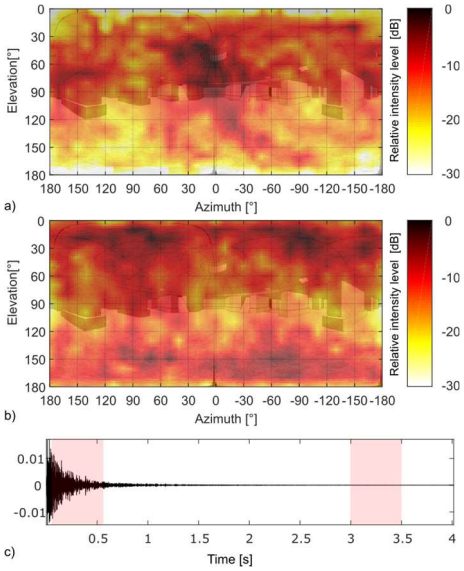

Fig. 10. Comparison between directional reflection maps at 500 Hz for combination S1-R11 at: a) 50 ms from direct sound 0.5 s time window; b) 3.0 s from direct sound 0.5 s time window. c) Impulse response (omnidirectional) with shaded areas indicating the time intervals used in a) and b). IR amplitude is expressed using arbitrary units.

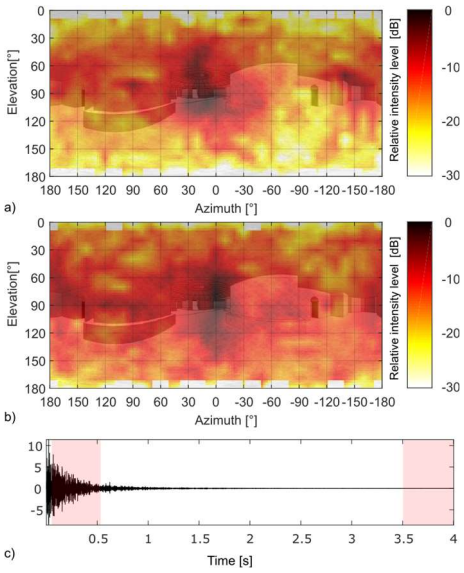

Fig. 11. Comparison between directional reflection maps at 500 Hz for combination S1-R8 at: a) 50 ms from direct sound 0.5 s time window; b) 3.0 s from direct sound 0.5 s time window. c) Impulse response (omnidirectional) with shaded areas indicating the time intervals used in a) and b). IR amplitude is expressed using arbitrary units.

Finally, combination S2-R8 was considered to represent the case when receivers are moved into the galleries. In this case the sound field distribution changed significantly as the early part (Fig. 11a) showed a clear dominance of reflections coming from the front (from the opening connecting to the rotunda) and from the back (reflecting back from the rear wall). Limited contribution of lateral reflections, and even more limited contributions from top and bottom surfaces, was observed because the loudest reflections arrived from the rotunda at grazing angles (very close to the direction of arrival of direct sound), while more diffuse reflections lost much of their energy after hitting several times the walls. In the late part (Fig. 11b) most of the acoustic energy kept arriving from the opening, but diffuse reflections were finally observed arriving from all directions.

To summarize, the analysis of the directional reflection maps allowed to conclude that the origin of the late decay at 500 Hz and above was the rotunda. However, the longer reverberation was due to a non-diffuse sound field caused by reflections between the floor and the dome, which are also the origin of the observed flutter echo. This late decay had a stronger initial energy when the source was in the rotunda (S2), and became weaker when the source was at the altar (S1), likely because the latter position caused direct sound to enter the rotunda with a grazing angle which caused a greater amount of acoustic energy being reflected towards the galleries, with lower and more scattered energy remaining in the rotunda, thus preventing flutter echoes to appear. When receivers were in the galleries the early sound came from the rotunda and spread initially along the main axis of the gallery. In the late part a diffuse field was finally observed, but the loudest reflections kept arriving from the opening, thus supporting the idea that the late decay originated from the rotunda. At the 2 kHz octave band, similar results were found, although characterized by increased diffusion of the sound field.

4. Discussion

At the end of the previous analysis of the measurements carried out in the crypt, it is possible to summarize the main findings, also trying to provide an explanation for each of them.

First of all, the directional intensity maps clarified that the longer reverberation time in the rotunda was due to a mostly mono-dimensional propagation between the floor and the vault. Such propagation appeared at selected receivers in the form of a clear flutter echo having a period of about 200 ms, depending on position. For combination S2-R11, with both source and receiver along the symmetry axis, the period was 185 ms, corresponding to a roundtrip path of 63 m. Along that direction, the distance between the opposite terminations of the galleries was about 45 m, corresponding to a longer period of 260 ms, but assuming that sound was reflected before entering the chapel such distance would reduce to 34 m, corresponding to a period of 200 ms. However, directional intensity maps clearly showed that points of origin of the fluttering reflections were the floor and the ceiling. A geometrical acoustic reconstruction of the reflection paths along the cross section was made to provide a simple qualitative explanation of how the flutter echoes can be generated by the curved surface of the vault, while showing that time periods may be quite long despite the limited height (Fig. 12). The analysis showed that adding up all the reflections yielded a roundtrip path of 53.3 m, corresponding to a period of 157 ms. This should be considered as the shortest period, as longer roundtrip paths (moving circularly) could be identified using a 3D model of the space.

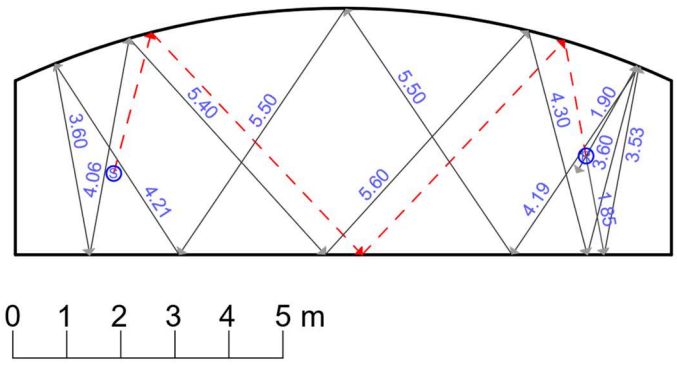

Fig 12. Schematic geometrical acoustic interpretation of the flutter echo appearing between source S2 and receiver R11. (– – –) propagation from source (S) to receiver (R), (——) roundtrip from (R) to (R).

Once this premise was made, the combined analysis of Bayesian methods and directional intensity maps showed different behaviours at different octave bands. A common feature to all measured responses was the presence of a steep initial decay followed by one or more, much weaker decays, with slower decay rates. Combination S2-R10 was a significant exception both in terms of initial decay (slower than others), and energy of the late decay (stronger than others, except at 125 Hz). Such steep initial decays observed in sub-volumes where no source was present contradicted the diffuse-field behaviour which was expected for such spaces (characterized by a concave shape and by an initial energy which is nearly zero). This suggested that a significant part of the direct sound was radiated into each sub-space, as if the source was right inside it. Then, the large opening and the repeated reflections between parallel surfaces caused a sudden drop of the acoustic energy, finally followed by the late reverberant sound coming from the rotunda.

At the 125 Hz octave band the observed double slope likely depended on coupling with the cathedral. In fact, the second decay had a reverberation time comparable with that of the cathedral. The initial decay was very similar in all the cases, except when both source and receiver were in the rotunda. In which case T1 was more than doubled compared to the other cases and, apart from a second slope appearing in S1-R10, no evidence of its propagation to galleries was found using Bayesian analysis. However, the shorter reverberation time in the rotunda (as compared to other octave bands), suggested the existence of some damping which also reduced the overall energy of that decay, thus making it less visible in the galleries. In fact, analysis of the spectrum measured in S2-R10 pointed out major peaks at 77 Hz, 115 Hz, and 155 Hz (easily explainable as axial modes along the z-axis, as the average height in the rotunda is 4.4 m), and spectral analysis carried out in S2-R2 pointed out similar resonance peaks, although only observed during the transition between the two decay processes.

At the 500 Hz octave band a rather complex picture appeared. For combination S2-R10 3D sound maps confirmed that the late decay (with T2=5.9 s) originated from the rotunda because of the floor-ceiling reflections, in combination with an initial decay (having T1=3.44 s) about 3 dB more energetic. The late decay appeared in all the other combinations, although with different, and generally much lower, energy. Consistently, the energy of the late decay process dropped when either the receiver was in a gallery, or the source was at the altar, and reached a minimum when source was at the altar and receiver was in a gallery. When source at the altar the excitation of the one-dimensional reflection pattern was less effective (being about 10 dB weaker) and the

sound field was slightly more diffuse. Under these conditions a third, but very weak, decay appeared, realistically due to sound energy coming back from the volume of the cathedral (as demonstrated by the very similar reverberation time).

Finally, at the 2 kHz octave band the combination of the different results was slightly closer to a "diffuse field" condition. In fact, in agreement with the behaviour predicted by SA equations for coupled volumes the late decay was mostly the same, independent of source position, and its energy consistently was at a maximum in the rotunda (particularly with the source in it), and decreased to a minimum when source was at the altar and receiver was in a gallery. However, the big difference between the energy of the first and second decay, suggested that while direct sound entered through the (comparatively) large gallery openings, a much lesser fraction of late sound got into them. Despite a slightly increased scattering, this was likely to depend, as observed at the 500 Hz octave band, on the vertical flutter echo, as sound kept on reflecting between floor and dome in the rotunda, and the fraction which was intercepted by the openings remained small.

5. Conclusions

The acoustics of the Crypt of the Cathedral of Cadiz was analysed in detail, starting from an on-site measurement campaign. The complex geometry of the space, made of a circular and domed central space (the rotunda) connected to six radial galleries (five of them very deep), and to the cathedral, originated an impressive collection of acoustic phenomena. Flutter echoes, non-diffuse sound propagation, double and triple slope decays were among the phenomena observed. Only the combined application of non-conventional methods of analysis, including Bayesian analysis and 3D sound maps, allowed us to identify and explain each of these phenomena. In summary, when sound is radiated in the rotunda it propagates into the galleries, thus being very rapidly absorbed by the many reflections taking place before sound can actually come back into the rotunda. Meanwhile, in the rotunda, a non-diffuse sound propagation is formed in which, due to its shape, sound travels between the floor and the dome for a long time causing audible flutter echoes. In this process, the mostly vertical propagation, emphasized by the lack of scattering elements on both surfaces, causes little late energy to reach the galleries which consequently show a second decay, having the same slope of the process in the rotunda, but with much less energy. Small variations occurred between the octave bands, with the notable exception of the 125 Hz octave band where, to complicate things, late sound coming from the cathedral masks the process originating from the rotunda. Further investigations are needed to clarify the origins of the complex phenomena discussed above, also involving on-site measurements of absorption coefficients of the different surfaces. Modelling of the coupled-space system is also under way but, considering the non-diffuse nature of the observed phenomena, also related to the presence of curved surfaces, setting up the correct parameters is a non-trivial task which requires a careful tuning.

Acknowledgments

The authors are very grateful to the Dean and the staff of the cathedral for their kind permission and assistance during the measurements. This research has been financially supported by ERDF funds and the Spanish Ministry of Economy and Competitiveness (MINECO) with reference BIA2014-56755-P.

References

[1] R. Johnson, E. Kahle, R. Essert, Variable coupled cubage for music performance, in Proc. Music and Concert Hall Acoustics, edited by Y. Ando and D. Noson (Academic Press, New York 1997), pp. 373-385.

[2] M. Ermann, M. Johnson, Exposure and materiality of the secondary room and its impact on the impulse response of coupled-volume concert halls, J. Sound Vib. 284 (2005) 915–931.

[3] J.Ch. Jaffe, Innovative approaches to the design of symphony halls, Acoust. Sci. Tech. 26 (2005) 240-243.

[4] N. Xiang, J. Summers, Acoustics in coupled rooms: modelling and data analysis, Proceedings of International Symposium on Room Acoustics, Satellite Symposium of the 19th International Congress on Acoustics, Seville, 10-12 September 2007.

[5] C.M. Harris, H. Feshbach, On the acoustics of coupled rooms, J. Acoust. Soc. Am. 22 (1950) 572–578.

[6] L. Cremer, H.A. Müller, Principles and Applications of Room Acoustics, vol. 1, trans. T. J. Schultz, Applied Science Publishers, New York, pp. 261-283, 1982.

[7] C. Thompson, On the acoustics of a coupled space, J. Acoust. Soc. Am. 75 (1984) 707–714.

[8] H. Kuttruff, Room Acoustics, 4th Ed., Spon Press, New York, 2000.

[9] J.E. Summers, R.R Torres, Y. Shimizu, Statistical-acoustics models of energy decay in systems of coupled rooms and their relation to geometrical acoustics, J. Acoust. Soc. Am. 116(2) (2004) 958-969.

[10] J.E. Summers, R.R. Torres, Y. Shimizu, Estimating midfrequency effects of aperture diffraction on reverberant-energy decay in coupled-room auditoria, Build. Acoust. 11(4) (2004) 271-291.

[11] J.E. Summers, Accounting for delay of energy transfer between coupled rooms in statistical-acoustics models of reverberant-energy decay, J. Acoust. Soc. Am. EL132 (2012) 129-134.

[12] A. Billon, V. Valeau, A. Sakout, J. Picaut, On the use of a diffusion model for acoustically coupled rooms, J. Acoust. Soc. Am. 120 (2006) 2043-2054.

[13] B.-I.L. Dalenbäck, Room acoustic prediction based on a unified treatment of diffuse and specular reflection, J. Acoust. Soc. Am. 100 (1996) 899-909.

[14] J.E. Summers, R.R. Torres, Y. Shimizu, B.-I.L. Dalenbäck, Adapting a randomized beam-axis-tracing algorithm to modelling of coupled rooms via late-part ray tracing, J. Acoust. Soc. Am. 118 (2005) 1491-1502.

[15] M. Ermann, Double sloped decay: Subjective listening test to determine perceptibility and preference, Build. Acoust. 14 (2007) 91–108.

[16] D.T. Bradley, L.M. Wang, The effects of simple coupled volume geometry on the objective and subjective results from nonexponential decay, J. Acoust. Soc. Am. 118 (2005)1480–1490.

[17] M. Ermann, Coupled volumes: Aperture size and the double-sloped decay of concert halls, Build. Acoust. 12 (2005) 1-14.

[18] ISO 3382-2, Acoustics-Measurement of room acoustic parameters-Part 2: Reverberation time in ordinary rooms, International Organisation for Standardisation, Geneva, Switzerland 2008.

[19] D.T. Bradley, L.M. Wang, Quantifying the double slope effect in coupled volume room systems, Build. Acoust. 16(2) (2009) 105–123.

[20] N. Xiang, P.M. Goggans, Evaluation of decay times in coupled spaces: Bayesian parameter estimation, J. Acoust. Soc. Am. 110 (2001) 1415–1424.

[21] N. Xiang, P.M. Goggans, Evaluation of decay times in coupled spaces: Bayesian decay model selection, J. Acoust. Soc. Am. 113 (2003) 2685–2697.

[22] N. Xiang, P.M. Goggans, T. Jasa, M. Kleiner, Evaluation of decay times in coupled spaces: Reliability analysis of Bayesian decay time estimation, J. Acoust. Soc. Am. 117(6) (2005) 3707-3715.

[23] N. Xiang, P. Goggans, T. Jasa, P. Robinson, Bayesian characterization of multiple-slope sound energy decays in coupled-volume systems, J. Acoust. Soc. Am. 129 (2011) 741–752.
[24] S. Anderson, M. Bratos-Anderson, Acoustic coupling effects in St. Paul's Cathedral, London, J. Sound Vib. 236 (2000) 209–225.
[25] F. Martellotta, Identifying acoustical coupling by measurements and prediction-models for St. Peter's Basilica in Rome, J. Acoust. Soc. Am. 126 (2009) 1175-1186.
[26] F. Martellotta, Understanding the acoustics of Papal Basilicas in Rome by means of a coupled-volumes approach, J. Sound Vib. 382 (2016) 413-427.
[27] Y. Chu, C.M. Mak, Early energy decays in two churches in Hong Kong, Appl. Acoust. 70 (2009) 579–587.
[28] F. Martellotta, A multi-rate decay model to predict energy-based acoustic parameters in churches, J. Acoust. Soc. Am. 125(3) (2009) 1281-1284.
[29] J. Kang, A method for predicting acoustic indices in long enclosures. Appl. Acoust. 51 (1997)169–80.
[30] D.S. Pavlovic, M. Mijic, The influence of absorption on statistical distribution of free path lengths in rooms. J. Acoust. Soc. Am. 123(5) (2008) 3497.
[31] H. Pu, H. Min, X. Qiu, J. Wang, On the sound field of a vault with two open ends, Appl. Acoust. 71 (2010) 556–563.
[32] A. Moreno, J. Zaragoza, F. Alcantarilla, Generation and suppression of flutter echoes in spherical domes, J. Acoust. Soc. Jpn. E2 (1981) 197-202.
[33] M.L.S. Vercammen, Sound concentration caused by curved surfaces, Technische Universiteit Eindhoven, 2012.
[34] F. Martellotta, On the use of microphone arrays to visualize spatial sound field information, Appl. Acoust. 74 (2013) 987-1000.
[35] ISO 3382-1, Acoustics–Measurement of room acoustic parameters -- Part 1: Performance spaces. ISO, Geneva, Switzerland, 2009.
[36] F. Martellotta, E. Cirillo, A. Carbonari, P. Ricciardi, Guidelines for acoustical measurements in churches, Appl. Acoust. 70 (2008) 378-388.
[37] L. Álvarez-Morales, T. Zamarreño, S. Girón, M. Galindo, A methodology for the study of the acoustic environment of Catholic cathedrals: application to the Cathedral of Malaga, Build. Environ. 72 (2014) 102-115.
[38] L. Álvarez-Morales, S. Girón, M. Galindo, T. Zamarreño, Acoustic Environment of Andalusian Cathedrals, Build. Environ. 103 (2016) 182−192.